Cellular Physiology and Biochemistry

Cell Physiol Biochem 2017;42:1177-1191
DOI: 10.1159/000478873
Published online: June 30, 2017
Accepted: April 19, 2017

© 2017 The Author(s)
Published by S. Karger AG, Basel
www.karger.com/cpb

Karger Open access

This article is licensed under the Creative Commons Attribution-NonCommercial-NoDerivatives 4.0 International License (CC BY-NC-ND) (http://www.karger.com/Services/OpenAccessLicense). Usage and distribution for commercial purposes as well as any distribution of modified material requires written permission.

Original Paper

Integrated High Throughput Analysis Identifies GSK3 as a Crucial Determinant of p53-Mediated Apoptosis in Lung Cancer Cells

Yu Zhang[a] Chenyang Zhu[a,b] Bangyao Sun[b] Jiawei Lv[a] Zhonghua Liu[a] Shengwang Liu[b] Hai Li[b]

[a]College of Life Science, Northeast Agricultural University, Harbin, [b]State Key Laboratory of Veterinary Biotechnology, Harbin Veterinary Research Institute, The Chinese Academy of Agricultural Sciences, Harbin, P. R. China

Key Words
p53 • GSK3 • Lung cancer • Apoptosis

Abstract
Background/Aims: p53 dysfunction is frequently observed in lung cancer. Although restoring the tumour suppressor function of p53 is recently approved as a putative strategy for combating cancers, the lack of understanding of the molecular mechanism underlying p53-mediated lung cancer suppression has limited the application of p53-based therapies in lung cancer. ***Methods and Results:*** Using RNA sequencing, we determined the transcriptional profile of human non-small cell lung carcinoma A549 cells after treatment with two p53-activating chemical compounds, nutlin and RITA, which could induce A549 cell cycle arrest and apoptosis, respectively. Bioinformatics analysis of genome-wide gene expression data showed that distinct transcription profiles were induced by nutlin and RITA and 66 pathways were differentially regulated by these two compounds. However, only two of these pathways, 'Adherens junction' and 'Axon guidance', were found to be synthetic lethal with p53 re-activation, as determined via integrated analysis of genome-wide gene expression profile and short hairpin RNA (shRNA) screening. Further functional protein association analysis of significantly regulated genes associated with these two synthetic lethal pathways indicated that GSK3 played a key role in p53-mediated A549 cell apoptosis, and then gene function study was performed, which revealed that GSK3 inhibition promoted p53-mediated A549 cell apoptosis in a p53 post-translational activity-dependent manner. ***Conclusion:*** Our findings provide us with new insights regarding the mechanism by which p53 mediates A549 apoptosis and may cast light on the development of more efficient p53-based strategies for treating lung cancer.

© 2017 The Author(s)
Published by S. Karger AG, Basel

Y. Zhang and C. Zhu contributed equally to this work.

Dr. Hai Li and Dr. Shengwang Liu

State Key Laboratory of Veterinary Biotechnology, Harbin Veterinary Research Institute, The Chinese Academy of Agricultural Sciences, No. 678, Heping road, Xiangfang district, Harbin 150069, Heilongjiang province, (P. R. China)
Tel. +86-451-51051700 / +86-451-51051698, E-Mail lihai@hvri.ac.cn / swliu@hvri.ac.cn

Introduction

Lung cancer is the leading cause of cancer-related death worldwide, with more than 1.8 million new cases and almost 1.6 million deaths estimated in 2012 [1]. More than one-third of the above mentioned new diagnoses were made in China [2]. Similar to other types of cancers, lung cancer is treated primarily with traditional therapies, such as surgery, radiation therapy, and chemotherapy. However, non-small cell lung cancer (NSCLC) and small cell lung cancer (SCLC), which represent more than 95% of all lung cancers, are not sensitive to chemotherapy or are only sensitive to chemotherapy at the early stage [3]. Thus, in addition to the aforementioned first-line treatments, epidermal growth factor receptor (EGFR) tyrosine kinase inhibitors (TKIs) are used to treat patients harbouring *EGFR* mutations or amplification.

Erlotinib (Tarceva) is currently the only EGFR-targeting agents approved by the FDA for NSCLC treatment [4]. Another first-generation EGFR TKI, gefitinib, demonstrated significant survival benefits in phase II trials, but not phase III trials, and therefore remains approved only for general use in Asia and for patients with tumours harbouring EGFR-activating mutations in Europe [5]. Moreover, cetuximab, an anti-EGFR mAb that has been approved for colorectal carcinoma and head-and-neck squamous cell carcinoma, is mentioned in several NSCLC treatment guidelines [6]. Despite exhibiting response rates greater than 60% and progression-free survival (PFS) and overall survival (OS) of more than one and two years, respectively, only 10% of NSCLCs in North America and Western Europe and approximately 30% to 50% of NSCLCs in East Asia harbour EGFR mutations [7]. Thus, identifying new therapeutic targets for lung cancer treatment is an important and urgent issue.

As lung cancer is associated with the dysregulation of signalling pathways associated with various cellular processes, such as cell cycle progression, cell proliferation and apoptosis, and angiogenesis, researchers have expended considerable effort to identify new agents capable of targeting these pathways as a means of achieving greater therapeutic benefits [8-10]. However, clinical trials have demonstrated that targeting these pathways individually exerts limited effects [11], which may be due to the heterogeneous nature of lung tumours. Additionally, numerous studies have shown that inhibiting a single target or pathway is an ineffective approach to treating cancer, which has given rise to the idea of using combinations of agents to target multiple signalling pathways simultaneously in order to combat lung cancer.

p53 is one of the most important tumour suppressors, as its inactivation is required for the development of almost all types of cancer [12]. An inactive version of the p53 protein is expressed in various cancers, which has given rise to the idea of using p53 re-activation to combat these cancers [13]. Profound *in vivo* suppression of various types of established tumours via p53 re-activation, without affecting normal tissues, was demonstrated by three independent studies in 2006 and 2007, supporting the idea that pharmacological p53 restoration may be an effective means of treating cancer [14-16]. According to the National Cancer Institute database, more than 150 clinical trials involving p53 are currently ongoing [17]. p53 gene therapy has been approved in China [18]. The most common mechanism underlying p53 dysfunction in human cancers is p53 dysregulation induced by the amplification of its negative regulators, such as the MDM2 and MDM4 (encoding MDMX) genes [19]. A recent study determined that the MDM2 309 T > G polymorphism is one of the most important factors associated with p53 downregulation and poor clinical outcomes in NSCLC patients; thus, this polymorphism may represent a promising target with respect to NSCLC treatment at the molecular level [20]. However, a study investigating the antitumour activities of the small-molecule MDM2 inhibitor RG7388 in lung cancer models observed only p53 pathway activation and cell proliferation inhibition, but not p53-mediated apoptosis [21]. It is well known that the biological outcomes of p53 activation vary, as they range from cell death to cell survival and are thus difficult to predict. To achieve the desired outcome of p53 activation with respect to lung cancer therapy, it is necessary to understand

the mechanism underlying p53-mediated lung cancer cell apoptosis to facilitate the efficient clinical application of p53-based therapies.

In the present study, we treated human NSCLC A549 cells with two well-known p53-reactivating compounds, nutlin [22] and RITA [23], to elucidate the mechanisms underlying p53-mediated lung cancer apoptosis. Using integrated analysis of genome-wide short hairpin RNA (shRNA) screening data in combination with genome-wide gene expression data, we identified GSK3 as one of the key factors in p53-mediated apoptosis in human lung cancer cells.

Materials and Methods

Cells and transfection

A549 cells were grown in Dulbecco's minimum essential medium (Sigma Aldrich, St. Louis, MO, USA) supplemented with 10% fetal calf serum (Invitrogen, Carlsbad, CA, USA), 10 U/ml penicillin/streptomycin (Sigma Aldrich) and 2 mM L-glutamine (Sigma Aldrich). The cells were treated for 8 hours for all molecular biology assays and for 24 hours for all FACS assays unless otherwise indicated. Small interfering RNAs (siRNA) for GSK3α were purchased from Qiagen (S100288554, Valencia, CA, USA). siRNAs for GSK3β (42839) and p53 (106141) and a negative-control siRNA (AM4611) were all purchased from Invitrogen. siRNA transfection was performed using Lipofectamine 2000 (Invitrogen) according to the manufacturer's instructions.

Reagents

PFT-α, PFT-μ, nutlin (Nutlin-3, CAS Number 548472-68-0), lithium chloride and propidium iodide (PI) were all purchased from Sigma. RITA, SB216763, TWS119 and AR-A014418 were purchased from Selleckchem (Selleck Chemicals, Houston, TX, USA).

Growth suppression assays

Fluorescence-activated cell sorting (FACS) was performed using a BD FACScan flow cytometer. Analysis was performed using a FACScan flow cytometer with CellQuest software, version 4.0.2 (BD, Mountain View, California, USA). Cell cycle assays were performed via FACS with PI staining, as described in [24]. Cell proliferation assays were performed via FACS with BrdU-PI staining (BrdU, Sigma-Aldrich; FITC-conjugated anti-BrdU antibody, ab74545, Abcam, MA, USA), according to the manufacturer's instructions. Apoptosis assays were performed via FACS with Annexin V-PI staining using an Annexin V-FITC Apoptosis Detection Kit (ab14085, Abcam) or sub-G1 population detection via PI staining according to the manufacturer's instructions.

RT-qPCR

Total RNA was isolated using Trizol (Invitrogen) and reverse-transcribed using a SuperScript III First-Strand Synthesis Kit (Invitrogen) according to the manufacturer's instructions. RT-qPCR was performed using a SYBR PrimeScriptTM Kit (TaKaRa Bio Inc, Tokyo, Japan) on an ABI 7500 Real-Time PCR System (Life Technologies, Inc., Carlsbad, CA, USA). The primer sequences are presented (for all online suppl. material, see www.karger.com/doi/000478873) in Table S1.

Protein extraction and Western blotting

Western blotting was performed as described in [25]. Briefly, cells were washed with ice-cold PBS and soluble proteins were extracted with cell lysis buffer (100 mM Tris-HCl pH=8, 150 mM NaCl, 1% NP-40, phosphatase and protease inhibitor cocktail tablets (Abcam) according to the manufacturer`s protocol). The protein concentration was determined using the Bio-Rad Bradford assay (Bio-Rad, Hercules, CA) and BSA standards (Sigma Aldrich). An equal amount of protein was separated by SDS-PAGE. The following antibodies were used: p53 (DO-1, Santa Cruz, St Jose, CA, USA), GSK3α (EP793Y, Abcam), GSK3β (Y174, Abcam), p-GSK3 (α/β) (Tyr279/Tyr216) (ab75745, Abcam), p-GSK3α (Ser21) (ab28808, Abcam), p-GSK3β (Ser9) (EPR2286Y, Abcam), and β-actin (Sigma Aldrich).

Luciferase assay

Cells were transiently co-transfected with the Renilla luciferase reporter vector (pGL4.77, Promega, Madison, WI) and empty plasmid (pGL4.27, Promega) or the plasmid containing TCF-LEF response element (pGL4.49, Promega) for 24 h using Lipofectamine 2000 (Invitrogen), followed by the administration of indicated GSK3 inhibitors for another 24 h. Then the luciferase activity in total cell lysates was measured using the Dual-Glo luciferase reporter assay (Promega), and data were calculated according to manufacturer instructions. Briefly, for each well, the ratio of firefly luminescence to Renilla luminescence was calculated. After that, the ratio of each experimental well was normalized to the ratio of background control well. Then the relative luciferase activity was determined as the ratio of normalized ratio of each inhibitor to that of DMSO control.

Table 1. List of top 20 upregulated genes and top 20 downregulated genes by nutlin treatment in A549 cells

Gene_id	Gene	Locus	Log2(fold_change)	p_value	q_value
Top 20 upregulated genes upon nutlin					
XLOC_046673	AC072052.7	7:6490792-6491098	∞	1.45E-036.44E-03	
XLOC_007248	SYT8	11:1828306-1837521	∞	5.00E-053.15E-04	
XLOC_010648	MUC19	12:40393394-40570832	7.13	5.00E-053.15E-04	
XLOC_029164	TP53I3	2:24076525-24201698	4.36	5.00E-053.15E-04	
XLOC_050171	LY6D	8:142784879-142812120	4.17	5.00E-053.15E-04	
XLOC_037227	SORCS2	4:7192537-7742836	4.08	5.00E-053.15E-04	
XLOC_030648	ABCA12	2:214810228-215138428	3.85	5.00E-053.15E-04	
XLOC_026188	CYP4F2	19:15878022-15898120	3.77	5.00E-053.15E-04	
XLOC_028882	INPP5D	2:233059966-233207903	3.67	5.00E-053.15E-04	
XLOC_021825	RNF157-AS1	17:76136332-76240373	3.64	3.05E-031.22E-02	
XLOC_025224	LGALS7B	19:38789210-38791749	3.53	5.00E-053.15E-04	
XLOC_042898	CDKN1A	6:36676459-36687339	3.47	5.00E-053.15E-04	
XLOC_054823	PRKY,RNU6-941P	Y:7273971-7381548	3.38	3.45E-031.35E-02	
XLOC_051307	CYSRT1	9:137224634-137226311	3.37	5.00E-053.15E-04	
XLOC_000130	RP3-510D11.2	1:9182006-9202619	3.28	5.00E-053.15E-04	
XLOC_044379	PTCHD4	6:47878027-48068689	3.11	5.00E-053.15E-04	
XLOC_037516	SPATA18	4:52051330-52097292	2.99	5.00E-053.15E-04	
XLOC_038724	RP11-241F15.1	4:49486925-49489554	2.95	9.40E-033.15E-02	
XLOC_023179	GRIN2C	17:74842022-74861504	2.80	5.00E-053.15E-04	
XLOC_037810	RP11-115D19.1	4:89551355-89841978	2.78	5.00E-053.15E-04	
Top 20 downregulated genes upon nutlin					
XLOC_017951	PIF1	15:64815631-64825668	-5.44	5.00E-053.15E-04	
XLOC_003859	FAM72C	1:143944178-143971965	-5.37	2.30E-039.58E-03	
XLOC_048171	ESCO2	8:27733310-27838095	-5.22	1.50E-048.63E-04	
XLOC_044116	MDC1	6:30699806-30717889	-5.03	5.00E-053.15E-04	
XLOC_022791	KIF18B	17:44924708-44947711	-5.00	5.00E-053.15E-04	
XLOC_011716	CDCA3	12:6839953-6852066	-5.00	5.00E-053.15E-04	
XLOC_040564	KIF20A	5:138139765-138213343	-4.97	5.00E-053.15E-04	
XLOC_040801	HMMR	5:163460202-163494058	-4.93	5.00E-053.15E-04	
XLOC_015755	DLGAP5	14:55148111-55191678	-4.81	5.00E-053.15E-04	
XLOC_004657	NEK2	1:211658656-211675630	-4.81	5.00E-053.15E-04	
XLOC_023706	SKA1	18:50374994-50394173	-4.75	5.00E-053.15E-04	
XLOC_038310	NEIL3	4:177309835-177362943	-4.71	5.00E-053.15E-04	
XLOC_030823	HJURP	2:233775678-233854566	-4.68	5.00E-053.15E-04	
XLOC_022133	AURKB	17:8204732-8210600	-4.64	5.00E-053.15E-04	
XLOC_033602	GTSE1	22:46296740-46330810	-4.63	5.00E-053.15E-04	
XLOC_045472	ANLN	7:36324220-36453791	-4.59	5.00E-053.15E-04	
XLOC_004121	IQGAP3	1:156525404-156572604	-4.56	5.00E-053.15E-04	
XLOC_039201	CCNA2	4:121801316-121823933	-4.55	5.00E-053.15E-04	
XLOC_020744	FAM64A	17:6444414-6556494	-4.55	5.00E-053.15E-04	
XLOC_007142	MKI67	10:128096658-128126385	-4.52	5.00E-053.15E-04	

RNA sequencing

Genome-wide A549 cell gene expression profiling was performed using RNA deep sequencing by Annoroad Gene Technology Co., Ltd (Beijing, China). Library construction was performed following the manufacturer's instructions provided by Illumina (San Diego, CA, USA). Samples were sequenced on an Illumina HiSeq 2500 instrument.

High-throughput data analysis

RNA sequencing data were analysed with a web-based tool, Galaxy [26]. Pathway analysis was performed using DAVID (gene-enrichment analysis using EASE Score, a modified Fisher exact p-value) [27]. Functional protein network analysis was performed using STRING [28].

Genome-wide pooled shRNA screening

We combined publicly available genome-wide pooled short hairpin RNA (shRNA) screening data from A549 cells transduced with the Systems Biosciences 200K shRNA lentiviral library and subsequently treated with nutlin [29] with our RNA sequencing data to perform integrated pathway analyses. The experimental procedure and data processing procedure are described in [24].

Statistics

The SPSS software package (SPSS for Windows, Release 13.0 for Windows, SPSS Inc., Chicago, IL, UAS) was used for statistical analysis. Data obtained from several experiments are reported as the mean ± standard deviation (SD). The difference between two groups was determined by Student's t-test. Analysis of two-way ANOVA with Bonferroni was employed for multi-group comparison. A p value less than 0.05 was considered significant.

Results

p53-mediated A549 cell apoptosis and cell cycle arrest have distinct transcriptional profiles

We tested the biological effects of two well-studied p53 activators, nutlin and RITA, in wild-type p53-expressing human lung carcinoma A549 cells, as shown in Fig. 1. The inductions of p53 by nutlin and RITA were observed by western blotting (Fig. 1A). RITA induced A549 cell apoptosis (Fig. 1A), but not cell cycle arrest (Fig. 1A), while nutlin induced cell cycle arrest, but not apoptosis (Fig. 1A). The p53-dependence of RITA-induced apoptosis and of nutlin-induced cell cycle arrest was confirmed by p53 depletion using siRNA (Fig. 1B). Furthermore, we found that the apoptosis induced by RITA-mediated p53 activation and the cell cycle arrest induced by nutlin-mediated p53 activation are transcription dependent, as both of these processes were completely inhibited by PFT-α, a chemical inhibitor of p53 transcriptional activity [30] (Fig. 1C). Therefore, we used A549 cells treated with RITA or nutlin as a model to identify the factors affecting p53-mediated A549 apoptosis.

Table 2. List of top 20 upregulated genes and top 20 downregulated genes by RITA treatment in A549 cells

Gene_id	Gene	Locus	Log2(fold_change)	p_value	q_value
Top 20 upregulated genes upon RITA					
XLOC_004888	RP4-597N16.4	1:235104179-235104609	∞	5.00E-05	1.79E-04
XLOC_013644	WI2-1528O10.1	13:114346166-114346637	∞	5.00E-05	1.79E-04
XLOC_015320	RP11-736N17.4	14:103139674-103141959	∞	5.00E-05	1.79E-04
XLOC_016747	RP11-265N6.3	15:42571926-42572433	∞	5.00E-05	1.79E-04
XLOC_028570	AC005037.1	2:200844239-200845461	∞	5.00E-05	1.79E-04
XLOC_030789	AC017104.4	2:231437100-231437421	∞	5.00E-05	1.79E-04
XLOC_049681	AC100823.1	8:73241423-73259502	∞	5.00E-05	1.79E-04
XLOC_028007	NT5DC4	2:112721485-112764677	7.54	3.70E-03	9.27E-03
XLOC_033742	TXNRD2	22:19875516-20016808	3.72	7.00E-04	2.06E-03
XLOC_054823	PRKY,RNU6-941P	Y:7273971-7381548	3.58	5.00E-03	1.22E-02
XLOC_042056	FGF1	5:142310426-142698070	3.35	2.00E-04	6.53E-04
XLOC_011718	RNU7-1	12:6942977-6946003	3.34	5.00E-05	1.79E-04
XLOC_026541	EID2B	19:39530989-39534422	3.26	2.50E-04	8.02E-04
XLOC_001692	FCER1G	1:161215233-161220699	3.22	5.00E-05	1.79E-04
XLOC_000417	GPR3	1:27392643-27395814	3.15	5.00E-05	1.79E-04
XLOC_034254	EMC3-AS1	3:9958716-10011209	3.11	5.00E-05	1.79E-04
XLOC_029164	TP53I3	2:24076525-24201698	2.99	5.00E-05	1.79E-04
XLOC_022134	LINC00324	17:8220641-8224043	2.98	5.00E-05	1.79E-04
XLOC_045390	HOXA-AS2	7:27106183-27157936	2.87	1.50E-04	5.01E-04
XLOC_044872	CTGF	6:131948175-132077393	2.77	5.00E-05	1.79E-04
Top 20 downregulated genes upon RITA					
XLOC_004902	RP4-580N22.2	1:235957878-235971825	-∞	6.45E-03	1.53E-02
XLOC_052465	RP13-297E16.4	X:1732583-1755985	-∞	2.05E-03	5.46E-03
XLOC_045947	AC002451.3	7:95596681-95613719	-∞	1.75E-03	4.75E-03
XLOC_011545	TMEM132B	12:125186835-125662377	-4.53	5.00E-05	1.79E-04
XLOC_045112	PARK2	6:161347419-163315492	-3.89	2.00E-04	6.53E-04
XLOC_005448	PRKG1	10:50991357-52314128	-3.73	7.00E-04	2.06E-03
XLOC_046029	MUC12	7:100969622-101018949	-3.68	1.15E-03	3.25E-03
XLOC_046124	FOXP2	7:114086326-114693772	-3.30	5.00E-05	1.79E-04
XLOC_003617	DPYD	1:97077742-97921049	-3.17	5.00E-05	1.79E-04
XLOC_038706	CORIN	4:47593997-47838106	-3.13	5.00E-05	1.79E-04
XLOC_017877	ALDH1A2	15:57953423-58569843	-3.11	5.00E-05	1.79E-04
XLOC_014936	RGS6	14:71932438-72595125	-3.08	5.00E-05	1.79E-04
XLOC_013004	GALNT9	12:132196371-132329349	-3.08	1.00E-04	3.44E-04
XLOC_044476	LGSN	6:63275950-63319977	-2.99	4.00E-04	1.23E-03
XLOC_048687	CPQ	8:96645226-97149654	-2.90	5.00E-05	1.79E-04
XLOC_013183	NBEA	13:34942286-35673022	-2.83	5.00E-05	1.79E-04
XLOC_021266	ZBTB7C	18:48026672-48110752	-2.79	5.00E-05	1.79E-04
XLOC_034431	ITGA9	3:37452114-37861780	-2.73	1.00E-03	2.86E-03
XLOC_007506	NAV2	11:19350723-20121598	-2.71	5.00E-05	1.79E-04
XLOC_036332	ABI3BP	3:100749155-100993515	-2.68	5.00E-05	1.79E-04

Because the apoptosis and cell cycle arrest induced by p53 activation are transcription dependent, we analysed the genome-wide gene expression profiles of RITA- or nutlin-treated A549 cells to compare the p53-mediated pro-apoptotic transcription profile and pro-cell cycle arrest transcription profile. Using RNA sequencing, we identified 658 upregulated genes and 797 downregulated genes reflecting the pro-apoptotic function of p53 reactivated by RITA and 319 upregulated genes and 568 downregulated genes reflecting the pro-cell cycle arrest effects of p53 reactivated by nutlin using the following criteria: (i) p value < 0.05,

(ii) q value < 0.05, and (iii) fold change > 2 (see supplementary material, Table S2 and S3). The top 20 upregulated genes and top 20 downregulated genes by nutlin or RITA treatment in A549 cells were listed in Table 1 and Table 2 respectively. Hierarchical clustering analysis involving these differentially expressed genes demonstrated efficient clustering of the biological replicates of control and RITA- or nutlin-treated cells (Fig. 2A). For validation purposes, the transcription levels of 20 randomly selected differentially expressed genes were determined via RT-qPCR. The RT-qPCR results were similar to those obtained with RNA-seq (Fig. 2B), indicating the success of the RNA-seq assay.

Our analysis showed that RITA, which induces apoptosis, and nutlin,

Table 3. List of top 20 SLNs

HUGO Gene Symbol	Log2 Fold Change	Adj. p-value	p-value	p(wZ)
MON1B	-40.53	4.51E-26	1.73E-292.67E-02	
SQSTM1 // C5orf45	-38.89	3.43E-02	2.65E-031.53E-02	
RPS20	-38.83	1.95E-02	1.22E-031.04E-02	
LYRM7	-38.01	4.35E-02	3.67E-037.25E-03	
POLK	-38.00	2.03E-04	3.91E-064.28E-03	
ICA1L	-37.85	1.84E-03	5.97E-052.40E-02	
BCL11A	-37.68	2.75E-05	3.56E-071.88E-03	
FBXO8	-37.66	5.95E-03	2.57E-043.94E-03	
WWC2	-37.31	4.27E-02	3.58E-031.64E-02	
POLK	-37.04	2.15E-02	1.39E-034.28E-03	
TNFAIP8L2	-36.88	1.81E-02	1.11E-031.91E-02	
SMOC1	-36.76	2.35E-02	1.57E-033.71E-02	
KDELR3	-36.70	5.35E-07	3.92E-093.28E-03	
ORAI3	-36.43	1.10E-05	1.23E-071.50E-02	
WDR72	-36.31	4.51E-02	3.86E-034.10E-02	
RRN3	-36.30	3.63E-05	4.91E-074.29E-02	
KCNMB4	-36.18	4.05E-02	3.32E-031.58E-02	
FNBP4	-36.16	3.40E-02	2.61E-033.12E-02	
ERCC8	-36.02	3.50E-04	7.78E-061.31E-03	
FAM126A	-36.02	3.50E-04	7.78E-062.62E-02	

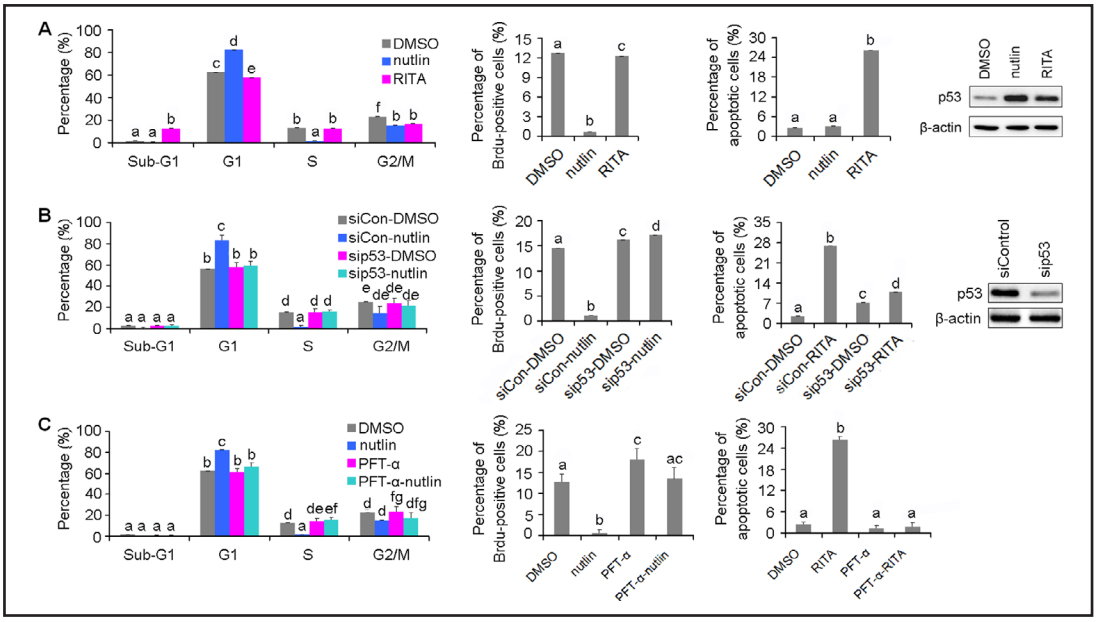

Fig. 1. A549 cells treated with RITA or nutlin was used as experimental model of p53-mediated suppression of lung cancer. (A) The biological outcomes of RITA and nutlin in A549 cells were determined by assessing cell cycle, cell proliferation and apoptosis. The induction of p53 in A549 cells upon nutlin or RITA treatment was assessed by immunoblotting (right panel). β-actin was used as loading control. (B) p53 dependence of the effect of RITA and nutlin was assessed in p53-depleted A549 cells. The depletion of p53 in A549 cells with siRNA targeting p53 was assessed by immunoblotting (right panel). β-actin was used as loading control. (C) The effect of RITA and nutlin was halted by blocking p53 transcriptional activity with PFT-α. Cell cycle was assessed by FACS using Propodium Iodide (PI) staining (left panels of A, B, and C), cell proliferation was assessed by FACS using Brdu-PI double staining (middle panel of A, and C, middle left panel of B), and apoptosis was assayed by FACS of Annexin V-PI-stained cells (right panel of A, and C, middle right panel of B) or sub-G1 population detection using PI staining (left panels of A, B, and C). Data are presented as mean ± SD, n = 3. One-way ANOVA with Bonferroni was employed and a p value less than 0.05 was considered significant. The values marked without the same superscript differ significantly.

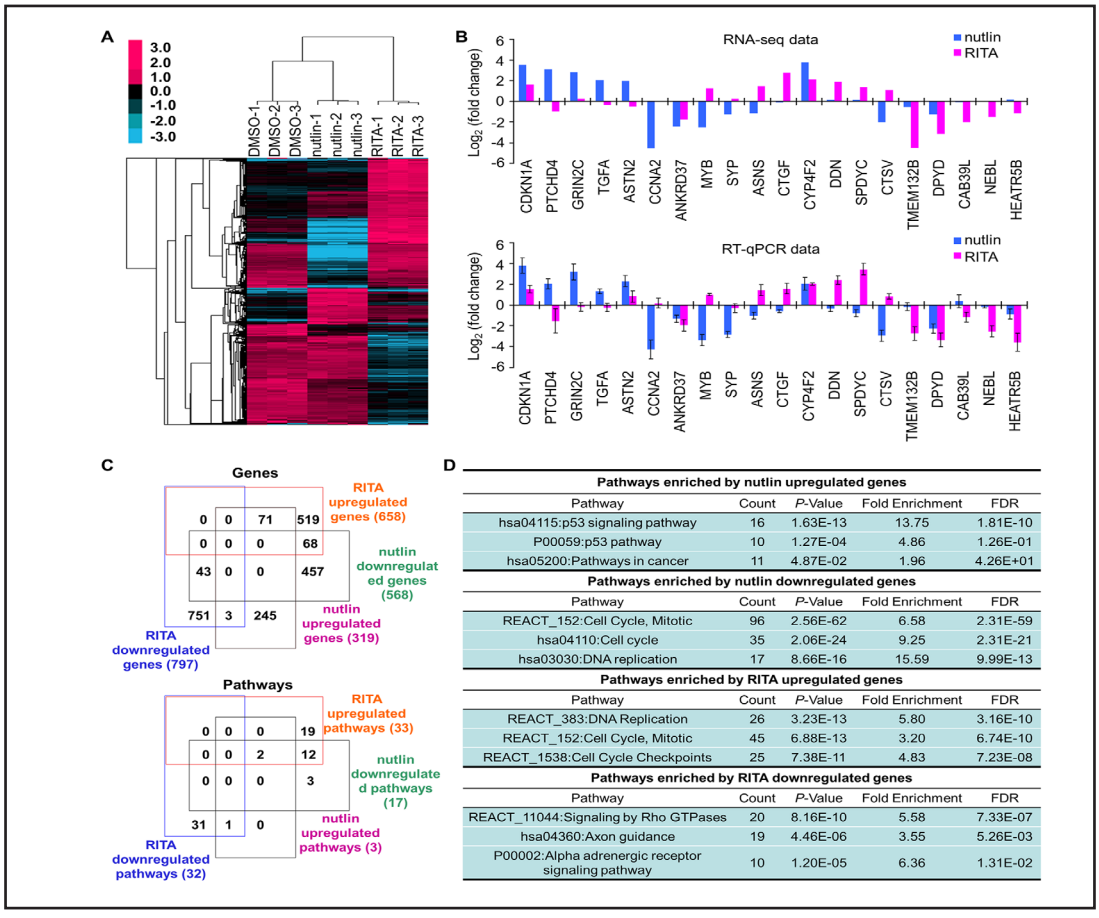

Pathways enriched by nutlin upregulated genes

Pathway	Count	*P*-Value	Fold Enrichment	FDR
hsa04115:p53 signaling pathway	16	1.63E-13	13.75	1.81E-10
P00059:p53 pathway	10	1.27E-04	4.86	1.26E-01
hsa05200:Pathways in cancer	11	4.87E-02	1.96	4.26E+01

Pathways enriched by nutlin downregulated genes

Pathway	Count	*P*-Value	Fold Enrichment	FDR
REACT_152:Cell Cycle, Mitotic	96	2.56E-62	6.58	2.31E-59
hsa04110:Cell cycle	35	2.06E-24	9.25	2.31E-21
hsa03030:DNA replication	17	8.66E-16	15.59	9.99E-13

Pathways enriched by RITA upregulated genes

Pathway	Count	*P*-Value	Fold Enrichment	FDR
REACT_383:DNA Replication	26	3.23E-13	5.80	3.16E-10
REACT_152:Cell Cycle, Mitotic	45	6.88E-13	3.20	6.74E-10
REACT_1538:Cell Cycle Checkpoints	25	7.38E-11	4.83	7.23E-08

Pathways enriched by RITA downregulated genes

Pathway	Count	*P*-Value	Fold Enrichment	FDR
REACT_11044:Signaling by Rho GTPases	20	8.16E-10	5.58	7.33E-07
hsa04360:Axon guidance	19	4.46E-06	3.55	5.26E-03
P00002:Alpha adrenergic receptor signaling pathway	10	1.20E-05	6.36	1.31E-02

Fig. 2. Analysis of RNA sequencing data revealed distinct transcriptional profiles by RITA and nutlin in A549 cells. (A) Heatmap representation of the expression profiles of genes significantly changed by RITA or nutlin in A549 cells. Red indicates promotion and blue indicates repression. Columns indicate arrays and rows indicate genes. Raw data was normalized within each row. p value < 0.05, q value < 0.05, and Fold change > 2. (B) The transcriptional level of 20 selected genes was examined by RT-qPCR and compared with RNA-seq data for validation. Data are presented as mean ± SD, n = 3. Student's t-test was employed for comparison and a p value less than 0.05 was considered significant. (C) Venn diagram shows the intersection of genes (upper panel) and pathways (lower panel) significantly changed by RITA or nutlin treatment in A549 cells. p< 0.05. (D) Top 3 pathways significantly enriched by RITA or nutlin upregulated/downregulated genes. p< 0.05.

which induces cell cycle arrest, were associated with distinct transcriptional profiles. Among 2157 differentially expressed genes, the two treatments had only 71 upregulated genes and 43 downregulated genes in common (Fig. 2C, upper panel). In addition, pathway analysis using the DAVID tool demonstrated that among the 3 and 17 pathways promoted and repressed by nutlin (see supplementary material, Table S4) and the 33 and 32 pathways promoted and repressed by RITA (see supplementary material, Table S5), only the p53 signalling pathway was commonly regulated by both treatments (Fig. 2C, lower panel). In contrast, 94.71% of the differentially expressed genes, which were enriched in 66 of the abovementioned 68 significantly altered pathways, were distinctly regulated by RITA or nutlin (Fig. 2C, lower panel). The top three pathways promoted or repressed by nutlin/RITA were listed in Fig. 2D.

Integrated genome-wide pathway analysis highlights key synthetic lethal nodes

To identify the molecular events responsible for the different biological outcomes induced by the aforementioned 66 pathways enriched by 2043 out of 2157 differentially

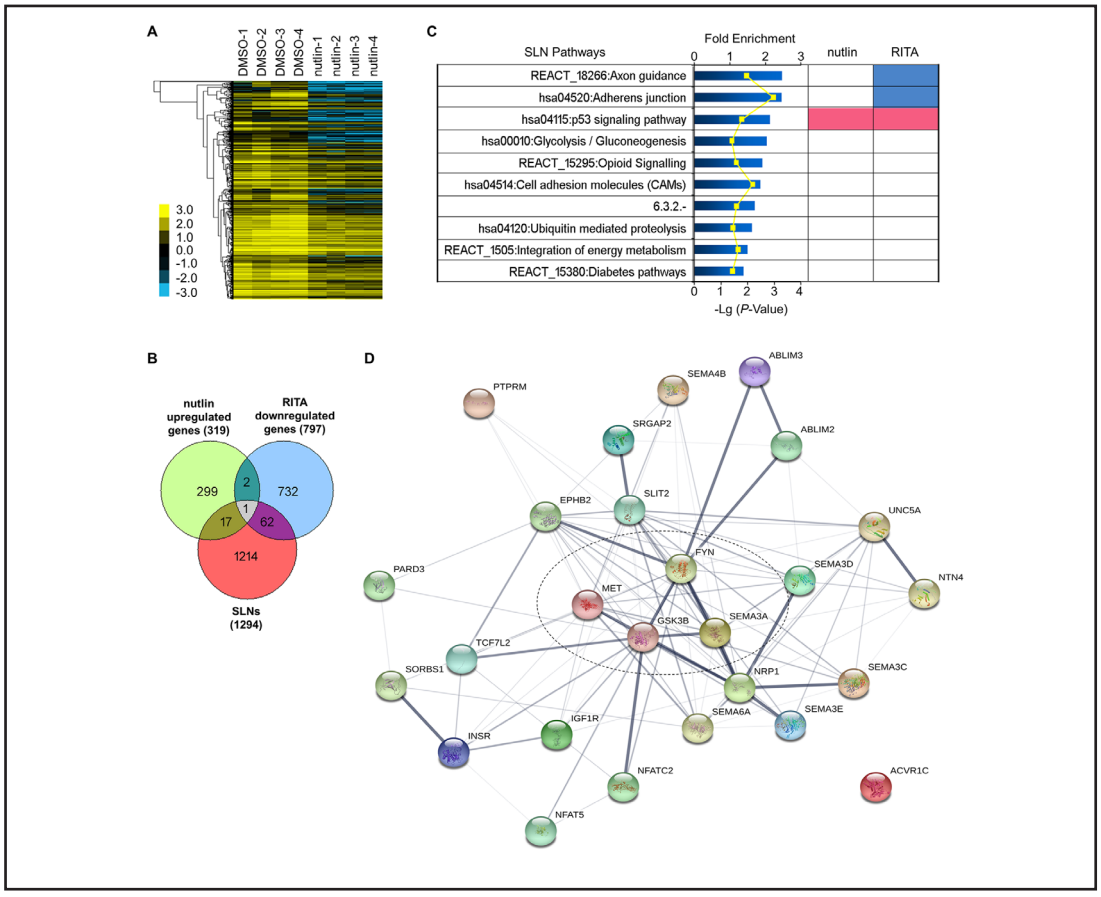

Fig. 3. Integrated genome-wide pathway analysis highlights key synthetic lethal nodes. (A) Hierarchical clustering analysis of the shRNA screen data identifies 1294 genes synthetic lethal (SLNs) with nutlin treatment in A549 cells. Yellow indicates low abundance of shRNA and blue reflects high abundance. Rows indicate shRNAs. Raw data was normalized within each shRNA. $p< 0.05$, Log_2 fold change > 1, and $p(wZ) < 0.05$. (B) Venn diagram shows the intersection of SLNs, nutlin induced genes and RITA repressed genes. (C) Combined pathway analysis with genome-wide shRNA screen data and transcription data. Synthetic lethal pathways enriched by 1294 SLNs after nutlin treatment are presented in the left part of the panel. The overlap of pathways identified by analysis of the genome-wide shRNA screen data and the RNA-seq data is shown in the right panel. Pink indicates the pathways enriched by induced genes; blue indicates the pathways enriched by repressed genes; white indicates the pathways enriched by neither repressed genes nor induce genes. $p< 0.05$. (D) Analysis of functional interactions between proteins encoded by the genes enriched in 'Adherens junction' and 'Axon guidance' pathways.

regulated genes acceptable for DAVID tool, we conducted integrated pathway analyses using our RNA-seq data and publicly available genome-wide shRNA screening data from A549 cells transduced with the Systems Biosciences 200K shRNA lentiviral library and subsequently treated with nutlin [29]. We identified 1294 genes that are synthetic lethal with nutlin whose knockdown could promote the cell killing effect of nutlin (Fig. 3A, and see supplementary material, Table S6), a few of which overlapped with genes that are significantly upregulated by nutlin or repressed by RITA (Fig. 3B). The top 20 genes synthetic lethal with nutlin treatment were listed in Table 3. The abovementioned 1294 genes that are synthetic lethal with nutlin were significantly enriched in 19 pathways (Fig. 3C), indicating that inhibition of these pathways is synthetic lethal with nutlin. Among these 19 pathways, two pathways, 'Adherens junction' and 'Axon guidance', were uniquely enriched by p53-downregulated genes and upon RITA treatment, but not by p53-upregulated genes or genes altered by nutlin

treatment, and none of the 19 pathways was uniquely enriched by p53-upregulated genes upon nutlin treatment. These data indicate the importance of the genes associated with these two pathways in p53-mediated A549 cell apoptosis induction.

Therefore, we subsequently performed an analysis of the functional connections among the proteins encoded by the 26 genes enriched in the 'Adherens junction' and 'Axon guidance' pathways upon RITA treatment using STRING software. Twenty-four of 26 genes had at least two connections, as shown in Fig. 3D. Notably, these 24 genes were centred on GSK3β, FYN, MET, and SEMA3A, of which only SEMA3A is a known tumour suppresser, having been identified in many types of tumours, including lung cancer [31-34]. Our genome-wide screening data showed that knocking down SEMA3A was not synthetic lethal with p53 activation in A549 cells (Table S6). Thus, SEMA3A was not considered for subsequent experiments. In contrast, GSK3β inhibition, FYN inhibition and MET inhibition have been shown as promising strategies for combating cancer [35-37]. In our study, both FYN inhibition and MET inhibition were synthetic lethal with p53 activation in A549 cells (Table S6). Although not synthetic lethal with p53 activation, according to the genomic screening data, GSK3β is well known to act upstream of FYN kinase [38], and GSK3β inhibition by either siRNA or chemical inhibitors has been shown to decrease MET activity levels in A549 cells [35]. Moreover, among GSK3β, FYN and MET, only GSK3β has been shown to bind p53 [39, 40] and to modulate p53-mediated apoptosis [41, 42]. The absence of GSK3β from the abovementioned list of synthetic lethal nodes may due to the high level of cell death that results from GSK3β inhibition [35] or to reductions in the levels of both the active and the inhibitory forms of GSK3β via knockdown [43]. We investigated GSK3β in subsequent experiments. Overall, our analysis indicated that GSK3β may serve as a crucial modulator of p53-mediated A549 cell apoptosis. We therefore investigated the effects of GSK3β on p53-mediated apoptosis upon nutlin treatment.

Pharmacological modulation of GSK3 promotes p53-induced apoptosis

First, we determined whether GSK3β depletion is synthetic lethal with nutlin-mediated p53 activation using siRNAs targeting GSK3β. Knockdown efficiency was evaluated by western blotting (Fig. 4A). Although GSK3β knockdown itself induced A549 cell apoptosis (Fig. 4B), GSK3β depletion had no additive effect on cell viability upon nutlin treatment (Fig. 4B). Similar results were obtained from GSK3α, which is 85% homologous to GSK3β and exhibits 98% homology in the kinase domains (Fig. 4C and D). Considering the redundancy between GSK3α and GSK3β, four well-used GSK3 inhibitors, lithium chloride, SB216763, TWS119 and AR-A014418, were employed in this study. Robust apoptosis was successfully triggered in nutlin-treated A549 cells by the administrations of three of the four GSK3 inhibitors which regulated phosphorylation states of GSK3α/β without affecting GSK3α/β protein levels (Fig. 4E and F), indicating the importance of specific post-translational modifications of GSK3 to the induction of A549 cell apoptosis in response to nutlin-mediated p53 re-activation. Among these inhibitors, only SB216763, failed to trigger apoptosis in A549 cells upon nutlin treatment (Fig. 4F). Given that GSK3α/β activity can be regulated by their activating phosphorylation (Tyr279 in GSK3α/Tyr216 in GSK3β) and inhibitory phosphorylation (Ser 21 in GSK3α/Ser 9 in GSK3β) [43], the effects of these GSK3 inhibitors on the phosphorylation state of GSK3α/β were compared. Western blotting revealed diverse phosphorylation patterns of GSK3 by these inhibitors (Fig. 4E). Consistent with the distinct effects of these inhibitors on the apoptosis of A549 cells in combination with nutlin treatment, comparing with the other three inhibitors, SB216763 is the only one having no profound inhibition on Tyr216 phosphorylation of GSK3β and induced the highest repression of Ser 9 phosphorylation of GSK3β in our experimental system (Fig. 4E), which indicated a potential pivotal role of GSK3β in the robust induction of apoptosis by these GSK3 inhibitors upon nutlin treatment. Among the three GSK3 inhibitors facilitating apoptosis in A549 cell upon nutlin treatment, TWS119 and AR-A014418 affected GSK3β and had no effect on GSK3α tyrosine phosphorylation. However, both inhibitors reduced not only the Tyr216 phosphorylation but also the Ser 9 phosphorylation of GSK3β (Fig. 4E),

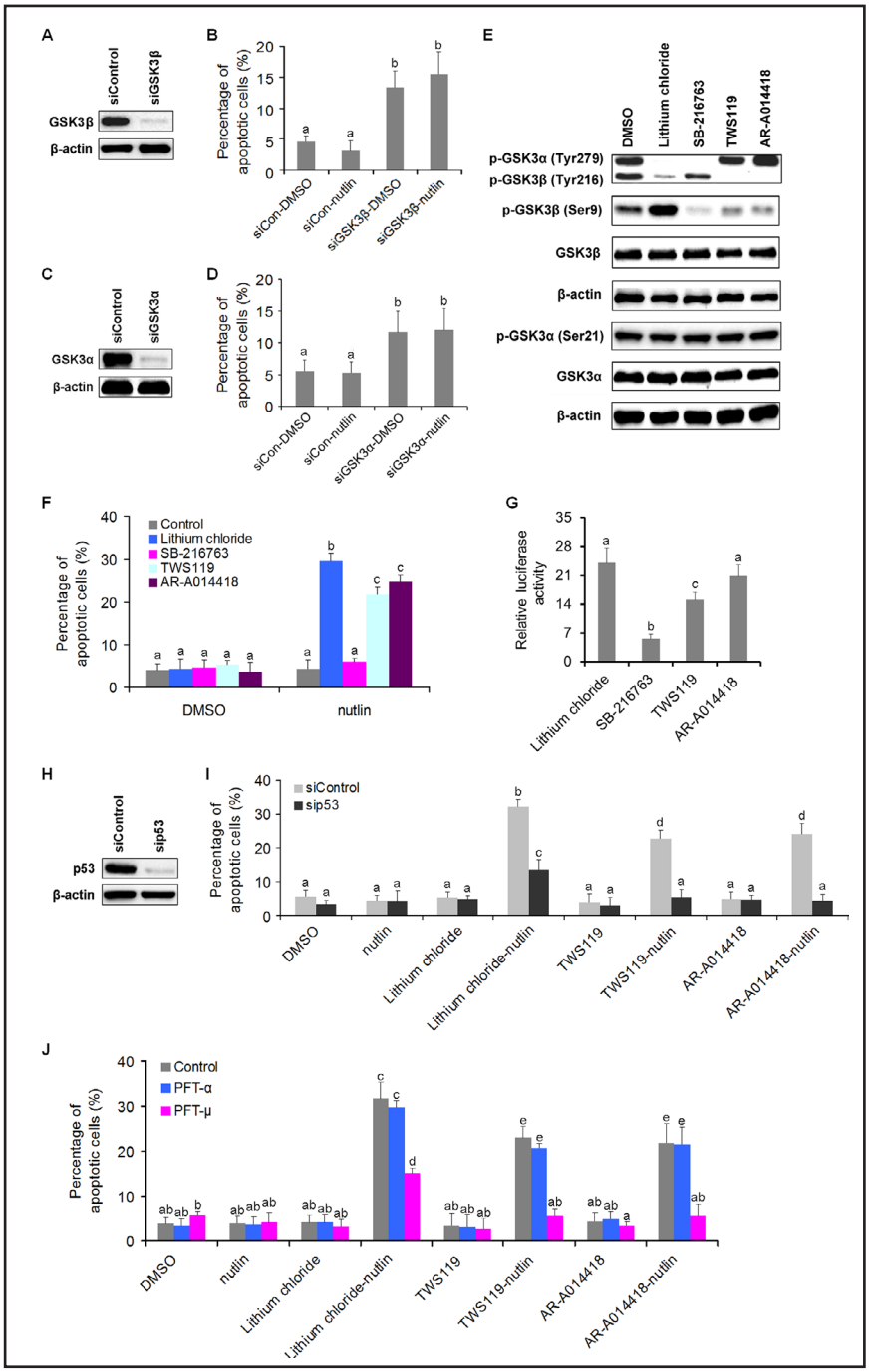

Fig. 4. Pharmacological modulation of GSK3β promotes p53-dependent apoptosis. (A, C) The depletions of GSK3β (A) andGSK3α (C) in A549 cells with siRNA targeting GSK3β or GSK3α were assessed by immunoblotting. β-actin was used as loading control. (B, D) The effect of GSK3β depletion (B) and GSK3α depletion (D) on apoptosis of A549 cells upon nutlin treatment was assessed by FACS performed as in Fig.1. (E) Protein levels of p-GSK3α/β (Tyr279/Tyr216, Ser21/Ser9) and total GSK3α/β in A549 cells with Lithium chloride, SB216763, TWS119 or AR-A014418 treatment were assessed by immunoblotting. (F) Effects of Lithium chloride, SB216763, TWS119 and AR-A014418 on apoptosis in A549 cells upon nutlin treatment were assessed by FACS performed as in Fig.1. (G) Assessment of the transcriptional activity of β-catenin after exposure to GSK3 inhibitors. Cells were transiently co-transfected with the Renilla luciferase reporter vector and empty plasmid or the plasmid containing TCF-LEF response element for 24h, followed by the administration of indicated GSK3 inhibitors for another 24h. Then the relative luciferase activity was measured and calculated. (H) The depletion of p53 in A549 cells with siRNA targeting p53 was assessed by immunoblotting. β-actin was used as loading control. (I) p53 dependence of the effects of Lithium chloride, TWS119 and AR-A014418 was assessed in p53-depleted A549 cells. (J) The effects of Lithium chloride, TWS119 and AR-A014418 were halted by blocking the post-transcriptional activity of p53 with PFT-μ instead of blocking p53 transcriptional activity with PFT-α. FACS data are presented as mean ± SD, n = 3. One-way (B, D) or two-way ANOVA (F, G, I and J) with Bonferroni was performed for multi-group comparison and a *p* value less than 0.05 was considered significant. The values marked without the same superscript differ significantly.

which made it hard to determine the effects of these two inhibitors on the activity of GSK3β. The activity of GSK3 can be directly reflected by the transcriptional activity of β-catenin, since GSK3 is a key kinase regulating Wnt signalling pathway through mediating β-catenin phosphorylation and subsequent degradation [44]. Therefore, the transcriptional activity of β-catenin upon the administration of each GSK3 inhibitor was detected using a luciferase reporter containing eight copies of TCF-LEF response element. Results showed that all these four inhibitors enhanced the transcriptional activity of β-catenin, while the transcriptional activity of β-catenin induced by SB216763 was much lower than that induced by other inhibitors (Fig. 4G). Given that Wnt signalling has been shown to confer the apoptotic effect of some GSK3 inhibitor in cancer cells [45], these results indicated that GSK3 inhibition is synthetic lethal with p53 re-activation, possibly through its effect on the action of Wnt signalling.

Furthermore, the additive apoptosis by TWS119 and AR-A014418 upon nutlin treatment was greatly attenuated by either p53-specific siRNA (Fig. 4H and I) or PFT-μ, a chemical inhibitor that halts p53 post-transcriptional activity by blocking p53 translocation into the mitochondria [46], but not by PFT-α, which inhibits p53 transcriptional activity by blocking p53 nuclear transport [29] (Fig. 4J), indicating that the pro-apoptotic effect of TWS119 and AR-A014418 on A549 cells upon nutlin treatment is p53 post-transcriptional activity-dependent, rather than p53 transcriptional activity-dependent. However, neither p53-specific siRNA nor p53 inhibitor could totally compromise the additive apoptosis by lithium chloride, which suppressed both GSK3α and GSK3β (Fig. 4E), upon nutlin treatment (Fig. 4H and I). This might due to the existence of additional mechanisms of the synthetic lethal effect of lithium chloride and nutlin.

Discussion

In the present study, we performed integrated genome-wide shRNA screening data analyses in combination with genome-wide gene expression analyses to elucidate the molecular mechanisms underlying p53-mediated lung cancer cell apoptosis. We identified GSK3 as one of the crucial determinants of p53-induced lung cancer cell apoptosis and demonstrated that the combination of GSK3 modulation and p53 activation induced by their specific targeting chemical compounds can trigger robust apoptosis in lung cancer cells.

Pharmacological re-activation of p53-mediated tumour suppression is a promising strategy for combating cancer. Several p53-reactivating compounds, including PRIMA-1, nutlin, RITA, tenovins and others, have been identified, and some of them are currently being tested in clinical trials [13]. However, the pleiotropic character of the p53 network makes it difficult to predict the consequences of p53 activation, which has limited the success of p53-based therapies. Gaining a better understanding of the mechanisms underlying p53-mediated apoptosis is urgently needed for the clinical application of p53-based therapies. To date, four genome-wide loss-of-function screens using pooled siRNA or shRNA libraries, including ours, have been carried out using human HCT116 colorectal cancer cells, MCF-7 breast carcinoma cells, and A549 lung carcinoma cells to identify the key factors and signalling pathways associated with p53-mediated tumour suppression [24, 29, 47, 48]. Genetic screening based on loss-of-function phenotypes could in principle reveal all factors and signalling pathways affecting the biological outcomes of pharmacological re-activation of p53. However, it is difficult to determine precisely which of these pathways confer the tumour suppressor function of p53 in response to specific stimuli. To answer this question, Sullivan et al. analysed genome-wide shRNA screening data from HCT116 colorectal cancer cells [29], and we analysed similar data from MCF-7 breast cancer cells [24], in combination with transcriptomic data. p53 is a promising therapeutic target in lung cancer treatment due to its frequent malfunction in human lung cancers, which is closely correlated with poor clinical outcomes in NSCLC patients [20]. Although Sullivan et al. also performed genome-

wide shRNA screening in A549 lung carcinoma cells, no transcriptomic data from A549 cells treated with p53-reactivating compounds are currently available. Thus we performed the RNA sequencing on A549 cells treated with p53-reactivating compounds and further analysed the transcriptomic data combined with genome-wide loss-of-function screening data, which may be useful to future studies.

Results from the studies, including the one performed by Sullivan et al. in HCT116 cells, our previous study in MCF-7 cells and present study in A549 cells, showed that most of the factors that modulate the tumour suppressor function of reactivated p53 are not affected by p53-reactivating compounds at transcriptional level. Additionally, according to our genome-wide shRNA screening data, most of the genes that are significantly regulated by pharmacological p53 re-activation are not synthetic lethal with p53 re-activation in A549 cells. Given that the functions of many of the factors that contribute to p53-mediated tumour suppression are regulated through control of their protein stability and posttranslational modifications rather than transcriptional modifications, identifying factors on the basis of only genome-wide shRNA screening data and gene expression data may not capture all the important participants in the tumour suppression function of pharmacological re-activation of p53. Thus, we compared the pathways enriched by the key nodes identified by genome-wide shRNA screening and the pathways enriched by the genes significantly altered by p53 activation according to the transcriptomic data in our previous study using MCF-7 cells and in this study using A549 cells. Using this strategy, in our previous study, we successfully determined that Sp1, which is modified at protein level, but not at transcriptional level, upon pharmacological p53 re-activation, is a key cofactor indispensable for the initiation of p53-mediated pro-apoptotic transcriptional repression and for robust apoptosis induction in both colorectal cancer cells and breast carcinoma cells [24]. In this study, we determined that GSK3 plays a key role in p53-mediated A549 cell apoptosis.

Surprisingly, this crucial role of GSK3 could only be identified by GSK inhibitors (Fig. 4F) but not by genome-wide shRNA screening (Table S6) or siRNA targeting GSK3α/β (Fig. 4B). This may due to the redundancy of the two isoforms or the requirement of the existence of GSK3 protein for successful induction of apoptosis upon p53 re-activation. Although GSK3α and GSK3β are 98% homology in the kinase domain and perform similar function in many biological processes, previous studies on colorectal cancer cells showed that GSK3β, but not GSK3α, binds to p53 and promotes p53-dependent apoptosis [40-42]. Besides, in our experimental system, the transcription level of GSK3β was differentially regulated by RITA (induces apoptosis in A549 cells) and nutlin (induces cell cycle arrest in A549 cells), whereas neither RITA nor nutlin altered the transcription level of GSK3α (Table S2 and S3). Further, the common difference between SB216763, which could not induce apoptosis in combination with p53 re-activation, and the other GSK3 inhibitors, which were synthetic lethal with p53 re-activation, are that SB216763 had less effect on Tyr216 phosphorylation of GSK3β (Fig. 4E and F) and induced lower level of beta catenin activity (Fig. 4G), compared with the other inhibitors. All these findings indicated a potential pivotal role of GSK3β, rather than GSK3α, in the robust induction of apoptosis by these GSK3 inhibitors upon nutlin treatment. Whereas, this hypothesis was not supported by the finding that lithium chloride, TWS119 and AR-A014418, which all facilitated apoptosis in combination with nutlin in A549 cells, exhibited opposite effects on phosphorylation of GSK3β at Ser9 (Fig. 4E). Therefore, it is hard to identify the factor conferring the synthetic lethal effect of GSK3 inhibition and p53 re-activation based on our current findings. Additionally, Wnt signalling has been shown to be important for the apoptotic effect of some GSK3 inhibitor in cancer cells [45], since GSK3 is a key kinase repressing Wnt signalling pathway through mediating β-catenin phosphorylation and subsequent degradation [44]. In present study, we found that the transcriptional activity of β-catenin induced by SB216763 was much lower than those induced by other inhibitors, although the transcriptional activity of β-catenin was enhanced by all these four inhibitors (Fig. 4G). These results indicate a potential pivotal role of the activation level of Wnt signalling in the induction of nutlin-mediated apoptosis by pharmacological inhibition of GSK3. Of cause, this finding cannot rule out the possibility of

the involvement of specific isoform or post-translational modification of GSK3α/β in p53-mediated apoptosis upon GSK3 inhibition. Further investigations of the post-translational modifications of GSK3α/β in combination with point mutation at each site are still needed to answer this question.

In conclusion, our study indicates that pharmacological modulation of GSK3 promotes p53-mediated lung cancer cell apoptosis upon nutlin treatment and thus may provide a guide for new and more efficient strategies for p53-GSK3-based cancer therapies.

Acknowledgements

This study was funded by the University Nursing Program for Young Scholars with Creative Talents in Heilongjiang Province (Grant No. UNPYSCT-2016010), the National Key Research and Development Project of China (Grant No. 2016YFD0500107-4), the Harbin Special Fund for Innovative Talents in Science and Technology (Grant No. 2016RAXYJ072), "The Elite Youth Program" of the Chinese Academy of Agricultural Sciences, the China Agriculture Research System (Grant No. CARS-41-K12), and the Special Fund for Agro-scientific Research in the Public Interest (Grant No. 201203056).

Disclosure Statement

The authors declare no conflict of interest.

References

1 Stewart BW, Wild CP (eds): World Cancer Report 2014. Lyon, France, WHO Press, 2014, Chapter1.1, pp 4-5.
2 Hong QY, Wu GM, Qian GS, Hu CP, Zhou JY, Chen LA, Li WM, Li SY, Wang K, Wang Q, Zhang XJ, Li J, Gong X, Bai CX, on behalf of the Lung Cancer Group of the Chinese Thoracic Society Chinese Alliance Against Lung Cancer: Prevention and management of lung cancer in China. Cancer 2015;121:3080-3088.
3 Pore MM, Hiltermann TJ, Kruyt FA: Targeting apoptosis pathways in lung cancer. Cancer Let 2013;332:359-668.
4 Shepherd FA, Rodrigues Pereira J, Ciuleanu T, Tan EH, Hirsh V, Thongprasert S, Campos D, Maoleekoonpiroj S, Smylie M, Martins R, van Kooten M, Dediu M, Findlay B, Tu D, Johnston D, Bezjak A, Clark G, Santabárbara P, Seymour L, National Cancer Institute of Canada Clinical Trials Group: Erlotinib in previously treated non-small-cell lung cancer. N Engl J Med 2005;353:123-132.
5 Thatcher N, Chang A, Parikh P, Rodrigues Pereira J, Ciuleanu T, von Pawel J, Thongprasert S, Tan EH, Pemberton K, Archer V, Carroll K: Iressa Survival Evaluation in Lung Cancer. Lancet 2005;366:1527-1537.
6 Blumenschein GR Jr, Paulus R, Curran WJ, Robert F, Fossella F, Werner-Wasik M, Herbst RS, Doescher PO, Choy H, Komaki R: Phase II study of cetuximab in combination with chemoradiation in patients with stage IIIA/B non-small-cell lung cancer: RTOG 0324. J Clin Oncol 2011;29:2312-2318.
7 Rosell R, Moran T, Queralt C, Porta R, Cardenal F, Camps C, Majem M, Lopez-Vivanco G, Isla D, Provencio M, Insa A, Massuti B, Gonzalez-Larriba JL, Paz-Ares L, Bover I, Garcia-Campelo R, Moreno MA, Catot S, Rolfo C, Reguart N, Palmero R, Sánchez JM, Bastus R, Mayo C, Bertran-Alamillo J, Molina MA, Sanchez JJ, Taron M, Spanish Lung Cancer Group: Screening for epidermal growth factor receptor mutations in lung cancer. N Engl J Med 2009;361:958-967.
8 Chen S, Li P, Li J, Wang Y, Du Y, Chen X, Zang W, Wang H, Chu H, Zhao G, Zhang G: MiR-144 inhibits proliferation and induces apoptosis and autophagy in lung cancer cells by targeting TIGAR. Cell Physiol Biochem 2015;35:997-1007.
9 Nie P, Hu W, Zhang T, Yang Y, Hou B, Zou Z: Synergistic Induction of Erlotinib-Mediated Apoptosis by Resveratrol in Human Non-Small-Cell Lung Cancer Cells by Down-Regulating Survivin and Up-Regulating PUMA. Cell Physiol Biochem 2015;35:2255-2271.

10 Wang L, Chen Z, An L, Wang Y, Zhang Z, Guo Y, Liu C: Analysis of Long Non-Coding RNA Expression Profiles in Non-Small Cell Lung Cancer. Cell Physiol Biochem 2016;38:2389-2400.
11 Larsen JE, Cascone T, Gerber DE, Heymach JV, Minna JD: Targeted Therapies for Lung Cancer: Clinical Experience and Novel Agents. Cancer J (Sudbury, Mass) 2011;17:512-527.
12 Vogelstein B, Sur S, Prives C: p53: The Most Frequently Altered Gene in Human Cancers. Nature Education 2010;3:6.
13 Selivanova G: Therapeutic targeting of p53 by small molecules. Semin Cancer Biol 2010;20:46-56.
14 Martins CP, Brown-Swigart L, Evan GI: Modeling the therapeutic efficacy of p53 restoration in tumors. Cell 2006;127:1323-1334.
15 Ventura A, Kirsch DG, McLaughlin ME, Tuveson DA, Grimm J, Lintault L, Newman J, Reczek EE, Weissleder R, Jacks T: Restoration of p53 function leads to tumour regression *in vivo*. Nature 2007;445:661-665.
16 Xue W, Zender L, Miething C, Dickins RA, Hernando E, Krizhanovsky V, Cordon-Cardo C, Lowe SW: Senescence and tumour clearance is triggered by p53 restoration in murine liver carcinomas. Nature 2007;445:656-660.
17 Cheok CF, Verma CS, Baselga J, Lane DP: Translating p53 into the clinic. Nat Rev Clin Oncol 2011;8:25-37.
18 Lane DP, Cheok CF, Lain S: p53-based Cancer Therapy. Cold Spring Harb Perspect Biol DOI:10.1101/cshperspect.a001222.
19 Perry ME: The Regulation of the p53-mediated Stress Response by MDM2 and MDM4. Cold Spring Harb Perspect Biol DOI:10.1101/cshperspect.a000968.
20 Javid J, Mir R, Julka PK, Ray PC, Saxena A: Association of p53 and mdm2 in the development and progression of non-small cell lung cancer. Tumour Biol 2015;36:5425-5432.
21 Hai J, Sakashita S, Allo G, Ludkovski O, Ng C, Shepherd FA, Tsao MS: Inhibiting MDM2-p53 Interaction Suppresses Tumor Growth in Patient-Derived Non-Small Cell Lung Cancer Xenograft Models. J Thorac Oncol 2015;10:1172-1180.
22 Vassilev LT, Vu BT, Graves B, Carvajal D, Podlaski F, Filipovic Z, Kong N, Kammlott U, Lukacs C, Klein C, Fotouhi N, Liu EA: *In vivo* activation of the p53 pathway by small-molecule antagonists of MDM2. Science 2004;303:844-848.
23 Issaeva N, Bozko P, Enge M, Protopopova M, Verhoef LG, Masucci M, Pramanik A, Selivanova G: Small molecule RITA binds to p53, blocks p53-HDM-2 interaction and activates p53 function in tumors. Nature medicine 2004;10:1321-1328.
24 Li H, Zhang Y, Ströse A, Tedesco D, Gurova K, Selivanova G: Integrated high-throughput analysis identifies sp1 as a crucial determinant of p53-mediated apoptosis. Cell Death Differ 2014;21:1493-1502.
25 Zhang Y, Li H, Wei R, Ma J, Zhao Y, Lian Z, Liu Z: Endothelial Cell Regulates Cardiac Myocyte Reorganization through β1-integrin Signalling. Cell Physiol Biochem 2015;35:1808-1820.
26 Blankenberg D, Von Kuster G, Coraor N, Ananda G, Lazarus R, Mangan M, Nekrutenko A, Taylor J: Galaxy: a web-based genome analysis tool for experimentalists. Curr Protoc Mol Biol DOI:10.1002/0471142727.mb1910s89.
27 Huang DW, Sherman BT, Lempicki RA: Systematic and integrative analysis of large gene lists using DAVID Bioinformatics Resources. Nature Protoc 2009;4:44-57.
28 Franceschini A, Szklarczyk D, Frankild S, Kuhn M, Simonovic M, Roth A, Lin J, Minguez P, Bork P, von Mering C, Jensen LJ: STRING v9.1: protein-protein interaction networks, with increased coverage and integration. Nucleic Acids Res 2013;41:D808-815.
29 Sullivan KD, Padilla-Just N, Henry RE, Porter CC, Kim J, Tentler JJ, Eckhardt SG, Tan AC, DeGregori J, Espinosa JM: ATM and MET kinases are synthetic lethal with nongenotoxic activation of p53. Nat Chem Biol 2012;8:646-654.
30 Komarov PG, Komarova EA, Kondratov RV, Christov-Tselkov K, Coon JS, Chernov MV, Gudkov AV: A chemical inhibitor of p53 that protects mice from the side effects of cancer therapy. Science 1999;285:1733-1737.
31 Hu ZQ, Zhou SL, Zhou ZJ, Luo CB, Chen EB, Zhan H, Wang PC, Dai Z, Zhou J, Fan J, Huang XW: Overexpression of semaphorin 3A promotes tumor progression and predicts poor prognosis in hepatocellular carcinoma after curative resection. Oncotarget DOI:10.18632/oncotarget.10104.
32 Chakraborty G, Kumar S, Mishra R, Patil TV, Kundu GC: Semaphorin 3A suppresses tumor growth and metastasis in mice melanoma model. PLoS One DOI: 10.1371/journal.pone.0033633.
33 Jiang H, Qi L, Wang F, Sun Z, Huang Z, Xi Q: Decreased semaphorin 3A expression is associated with a poor prognosis in patients with epithelial ovarian carcinoma. Int J Mol Med 2015;35:1374-1380.

34 Zhou H, Wu A, Fu W, Lv Z, Zhang Z: Significance of semaphorin-3A and MMP-14 protein expression in non-small cell lung cancer. Oncol Lett 2014;7:1395-1400.
35 Remsing Rix LL, Kuenzi BM, Luo Y, Remily-Wood E, Kinose F, Wright G, Li J, Koomen JM, Haura EB, Lawrence HR, Rix U: GSK3 alpha and beta are new functionally relevant targets of tivantinib in lung cancer cells. ACS Chem Biol 2014;9:353-358.
36 Kim AN, Jeon WK, Lim KH, Lee HY, Kim WJ, Kim BC: Fyn mediates transforming growth factor-beta1-induced down-regulation of E-cadherin in human A549 lung cancer cells. Biochem Biophys Res Commun 2011;407:181-184.
37 Agwa ES, Ma PC: Targeting the MET receptor tyrosine kinase in non-small cell lung cancer: emerging role of tivantinib. Cancer Manag Res 2014;6:397-404.
38 Jain AK, Jaiswal AK: GSK-3beta acts upstream of Fyn kinase in regulation of nuclear export and degradation of NF-E2 related factor 2. J Biol Chem 2007;282:16502-16510.
39 Watcharasit P, Bijur GN, Song L, Zhu J, Chen X, Jope RS: Glycogen synthase kinase-3beta (GSK3beta) binds to and promotes the actions of p53. J Biol Chem 2003;278:48872-48879.
40 Eom TY, Jope RS: GSK3 beta N-terminus binding to p53 promotes its acetylation. Mol Cancer DOI:10.1186/1476-4598-8-14.
41 Ghosh JC, Altieri DC: Activation of p53-Dependent Apoptosis by Acute Ablation of Glycogen Synthase Kinase-3β in Colorectal Cancer Cells. Clin Cancer Res 2005;11:4580-4588.
42 Tan J, Zhuang L, Leong HS, Iyer NG, Liu ET, Yu Q: Pharmacologic modulation of glycogen synthase kinase-3beta promotes p53-dependent apoptosis through a direct Bax-mediated mitochondrial pathway in colorectal cancer cells. Cancer Res 2005;65:9012-9020.
43 Doble BW, Woodgett JR: GSK-3: tricks of the trade for a multi-tasking kinase. J Cell Sci 2003;116:1175-1186.
44 Peifer M, Pai LM, Casey M: Phosphorylation of the Drosophila adherens junction protein Armadillo: roles for wingless signal and zeste-white 3 kinase. Dev Biol 1994;166:543-556.
45 Duffy DJ, Krstic A, Schwarzl T, Higgins DG, Kolch W: GSK3 inhibitors regulate MYCN mRNA levels and reduce neuroblastoma cell viability through multiple mechanisms, including p53 and Wnt signalling. Mol Cancer Ther 2014;13:454-467.
46 Strom E, Sathe S, Komarov PG, Chernova OB, Pavlovska I, Shyshynova I, Bosykh DA, Burdelya LG, Macklis RM, Skaliter R, Komarova EA, Gudkov AV: Small-molecule inhibitor of p53 binding to mitochondria protects mice from gamma radiation. Nat Chem Biol 2006;2:474-479.
47 Berns K, Hijmans EM, Mullenders J, Brummelkamp TR, Velds A, Heimerikx M, Kerkhoven RM, Madiredjo M, Nijkamp W, Weigelt B, Agami R, Ge W, Cavet G, Linsley PS, Beijersbergen RL, Bernards R: A large-scale RNAi screen in human cells identifies new components of the p53 pathway. Nature 2004;428:431-437.
48 Brummelkamp TR, Fabius AW, Mullenders J, Madiredjo M, Velds A, Kerkhoven RM, Bernards R, Beijersbergen RL: An shRNA barcode screen provides insight into cancer cell vulnerability to MDM2 inhibitors. Nat Chem Biol 2006;2:202-206.